1296. Study on the non-uniform contact between the shaft-taper hole and toolholder for a high speed spindle

Shin-Yong Chen[1], I-Feng Lin[2]
[1]Department of Automation and Control Engineering, Far-East University, Tainan, Taiwan, R. O. C.
[2]Department of Mechanical Engineering, Far-East University, Tainan, Taiwan, R. O. C.
[1]Corresponding author
E-mail: [1]*sychen88@cc.feu.edu.tw*, [2]*lin.paton@msa.hinet.net*

(Received 9 April 2014; received in revised form 6 June 2014; accepted 16 June 2014)

Abstract. The drawbar mechanism of a motor built-in high speed spindle with ATC is to provide the clamping force to grip the toolholder for high speed cutting. The connection status between the shaft-taper hole and toolholder is important on the spindle design and manufacture. In this paper, contact analyses of the toolholder and shaft-taper hole using contact elements are conducted. The stresses distribution between the toolholder and shaft-taper hole is then obtained and is used for the subsequent finite element modal analysis. The finite element modal analysis results are verified by the experimental modal testing to guarantee the accuracy of finite element model. Non-uniform contact conditions between the shaft-taper hole and toolholder is addressed especially in this study. Different intensities of resistance to the cutting torque due to different clamping forces, coefficients of friction, contact types and contact rates are provided. The deformations on the shaft and toolholder are also studied in this paper. The results are helpful to design a motor built-in high speed spindle with a suitable clamping force for providing the necessary torque to resist the cutting force and to give a suggestion on the manufacture of toolholder and shaft-taper hole.

Keywords: motor built-in high speed spindle with ATC, shaft-toolholder system, clamping force, non-uniform contact.

1. Introduction

High speed cutting by using a CNC milling machine with a high speed spindle is a very well-known technology. Motor built-in high speed spindle with ATC is a major unit of CNC milling machine. The spindle provides the required torque to resist the cutting force. The connection status between the spindle and toolholder will be having great impact in the machining efficiency and accurate. Therefore, it is important to establish a rational finite element model for the static and dynamic analyses of the spindle. Hughes etc. [1] proposed a finite element method (FEM) for a class of contact-impact problems. Several sample problems were presented which demonstrate the accuracy and versatility of the analysis algorithm. Oysu [2] proposed a test example in a separate analysis using the FEM or using the Lagrange multiplier approach combined with FEM. The results obtained from both of methods are similar. However, the latter analysis speed was faster than the former. Gonza'lez [3] presented a unified formulation for the combination of the FEM and the boundary element method (BEM) in 3D frictional contact problems that is based on the use of localized Lagrange multipliers. This methodology provided a partitioned formulation which preserves software modularity and facilitates the connection of non-matching FE and BE meshes. Ju etc. [4] developed a new contact element based on penalty function method for frictional contact problems in finite element analysis (FEA). The novel advantage of this new algorithm is that the contact element stiffness matrix is symmetric, even for frictional contact problems with a large sliding mode. The results using this new element are virtually identical to those obtained using conventional unsymmetrical contact element stiffness matrix. However, FEA using this new contact element requires only 1/2 computing time and storage space of those using unsymmetrical contact elements. Ezawa etc. [5] designed to improve the accuracy of analysis using the hybrid method combining FEM and BEM. Furthermore, the penalty function is applied to introduce the contact conditions. By considering the application to

general slide movements, a new eight-node contact element has been developed. Results confirm the validity and the accuracy of this method. The penalty function method is suitable for large distorted elements, friction, and augmented Lagrangian algorithm.

On the other hand, regenerative chatter is a well-known machining problem that results in unstable cutting process, poor surface quality and reduced material removal rate. This undesired self-excited vibration problem is one of the main obstacles in utilizing the total capacity of a machine tool in production. In order to obtain a chatter-free process on a machining center, stability diagrams were used by Ertürk etc. [6]. Their study presents an analytical method that uses Timoshenko beam theory for calculating the tool point FRF of a given combination by using the receptance coupling and structural modification methods to develop a reliable mathematical model to predict tool point FRF in a machining center and to make use of this model in studying the effects of individual bearing and contact parameters on tool point FRF. The model is also used to study the effects of several spindle, toolholder and tool parameters on chatter stability, and is verified by comparing the natural frequencies of a spindle-toolholder-tool assembly obtained from the model with those obtained from finite element software. Ertürk etc. [7] studied the effects of spindle-toolholder and toolholder-tool interface dynamics, as well as the effects of individual bearings on the tool point FRF by using their recently developed analytical model for predicting the tool point FRF of spindle-toolholder-tool assemblies. Some conclusions are made in this paper that bearing dynamics control the rigid body modes of the assembly, whereas, spindle-toolholder interface dynamics mainly affects the first elastic mode, while toolholder-tool interface dynamics alters the second elastic mode. Individual bearing and interface translational stiffness and damping values control the natural frequency and the peak of their relevant modes, respectively. Based on the effect analysis carried out, a systematic approach is suggested for identifying bearing and interface contact parameters from experimental measurements. In the contact studies for the high speed spindle, the major objects are mostly concentrated in dynamic analysis of spindle and functional design [8-16]. Only few studies are addressed on the contact behavior between the shaft-taper hole and the toolholder. Namazi etc. [17] proposed a majority of the chatter vibrations in high-speed milling originate due to flexible connections at the toolholder-spindle, and tool-toolholder interfaces. The toolholder-spindle taper contact is modeled by uniformly distributed translational and rotational springs. The springs are identified by minimizing the error between the experimentally measured and estimated frequency response of the spindle assembly. The paper also presents identification of the spindle's dynamic response with a toolholder interface, and its receptance coupling with the toolholder-tool stick out which is modeled by Timoshenko beam elements. The proposed methods allow prediction of FRFs at the tool tip by receptance coupling of tool and toolholder to the spindle, as well as analyzing the influence of relative wear at the contact by removing discrete contact springs between the toolholder and spindle. Sun etc. [18] proposed a dynamic analysis and static analysis method to design for the dimension of high speed spindle system HSK-Clamping-Unit/Form 63F. The tooling steel was utilized to model the drawbar shaft, clamping cone, gripper and hollow-shaft-taper parts. The FEA software, "ANSYS", was used to design the clamping system for getting better clamping force by change the structure of the clamping system. Hwang etc. [19] concentrated on the type synthesis of the tool-toolholder device, and the analysis of the mechanical advantage for the tool-toolholder device, and the development of a new drawbar system. The design techniques to develop a complete new drawbar are illustrates. Chen etc. [20, 21] proposed a key factor in designing a motor-built-in high speed spindle is to assemble the rotor-shaft by means of hot-fit. This paper presents a study of the influence of the hot-fit rotor on the local stiffness of the shaft. The dynamic analyses of the hot-fit rotor-shaft assembly using contact elements were conducted. The results obtained from this study indicate that the method is accurate and effective in analyzing the dynamic behavior of the rotary shaft system with hot-fit components by using contact elements.

The motor built-in high speed spindle is one of the key technologies for the precision manufacture. Make a comprehensive survey of the domestic and foreign researches, the spindle was studied by using the finite element analysis. However, there is no investigation on the

corresponding relationship which is important for the machining efficiency and accuracy between the toolholder and shaft-taper hole. In our previous study [22], the analysis of shaft-toolholder assembly with complete contact condition was investigated using contact element. The clamping force and the coefficient of friction have significant effects on the frictional torque. In this paper, non-uniform contact conditions between the shaft-taper hole and toolholder with different contact types and contact rates will be studied especially.

2. Analysis and verification approaches for the study

In this study, the shaft-toolholder structure is modeled and analysis by using ANSYS. In order to understand the frictional torque provided by shaft and toolholder under non-uniform contact conditions, the modeling is constructed with contact element. This study adopts 3D surface-to-surface model to study the dynamic characters of a shaft-toolholder assembly. In the analysis process, a stationary shaft-toolholder system is assumed and the contact element theory is used to analysis the normal force on the surface of shaft-taper hole. The normal force distribution on the cone surface is not uniform, since the normal force on the cone surface will change due to different cross-section area. The normal force is larger as the cross-section area is smaller. The normal force is inversely proportional to the cross-section area. After the normal force is calculated by FEA, the surface friction force can be obtained by multiply normal force of node at the cone surface with the friction coefficient μ. The surface friction force between the shaft-taper hole and toolholder is to provide the necessary torque to resist the cutting force. In this study, the friction torque provided by the surface friction force between the shaft-taper hole and toolholder can be obtained by multiply surface friction force of node at the cone surface with the sectional radius as shown in Fig. 1. In Fig. 1, black dot labelled with i is denoted as ith cross section of the cone, L the length of the cone, α the angle of the cone. The detailed discussion on the calculation of surface friction force can be found in [22]. The calculation of total frictional torque (T_f) can be summarized as:

$$T_f = \left[(f_{11} + f_{12} + \cdots + f_{1n})r_1 + \cdots + (f_{i1} + f_{i2} + \cdots + f_{ij} + \cdots + f_{in})r_i + \cdots + (f_{m1} + f_{m2} + \cdots + f_{mn})r_m\right], \quad (1)$$

where m is the number of cross section when the cone is meshed, n the number of node for each cross section, f_{ij} the surface friction force of jth node of ith cross section, which is in the tangential direction, and r_i the radius of ith cross section.

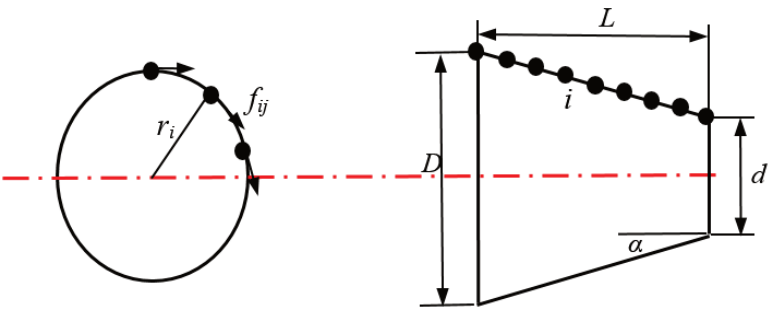

Fig. 1. The calculation of the frictional torque

Because of the machining inaccuracy of the taper of the toolholder and/or shaft-taper hole, the contact will not be complete. Therefore, two contact types as shown in Fig. 2 are designed to simulate the non-uniform contact conditions. One of both types is the contact region at larger diameter (referred to as Type I) and another is at smaller diameter (referred to as Type II). Four contact rates are assigned as 70 %, 80 %, 90 % and 100 % in this study.

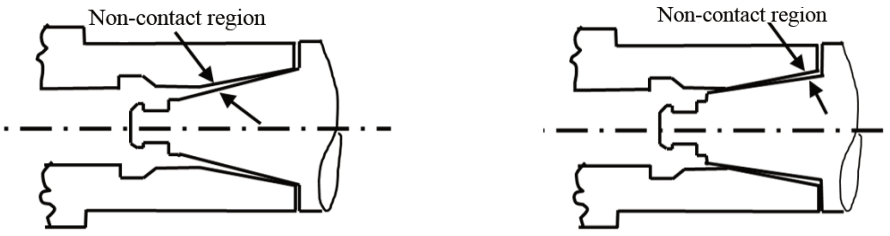

Fig. 2. Schematic of non-uniform contact conditions: a) contact region at larger diameter (Type I); b) contact region at smaller diameter (Type II)

On the other hand, in order to verify the accuracy of the constructed finite element model, the finite element modal analysis is performed to obtain the natural frequencies and is verified with those obtained from modal testing firstly. Fig. 3 shows the schematic of experiment modal testing apparatus. The boundary condition of the specimen used for the modal testing is of "soft suspension" and is an approximately ideal free-free boundary condition. Generally, it is infeasible to reach a condition of free vibration in a modal testing; soft suspension therefore becomes a reasonable approach. In this study, the shaft-toolholder system is suspended with rubber bands in the modal testing. In the specimen of the test, an accelerometer is attached to the shaft-toolholder system at location 13 as shown in Fig. 3. The 15 locations as marked 1 through 15 in Fig. 3 are the locations, each of which a hammer is used to create excitation. A modal testing aims at assuring modal parameters including natural frequencies, mode shapes, and damping ratios. The mode shapes corresponding to the natural frequencies are obtained based on the frequency response functions (FRFs) derived at pre-selected locations of the tested specimen. In this study, a SigLab spectrum analyzer is used to obtain the fifteen measured FRFs and the ME'scopeVES software is then used to estimate the natural frequencies and mode shapes corresponding to the natural frequencies.

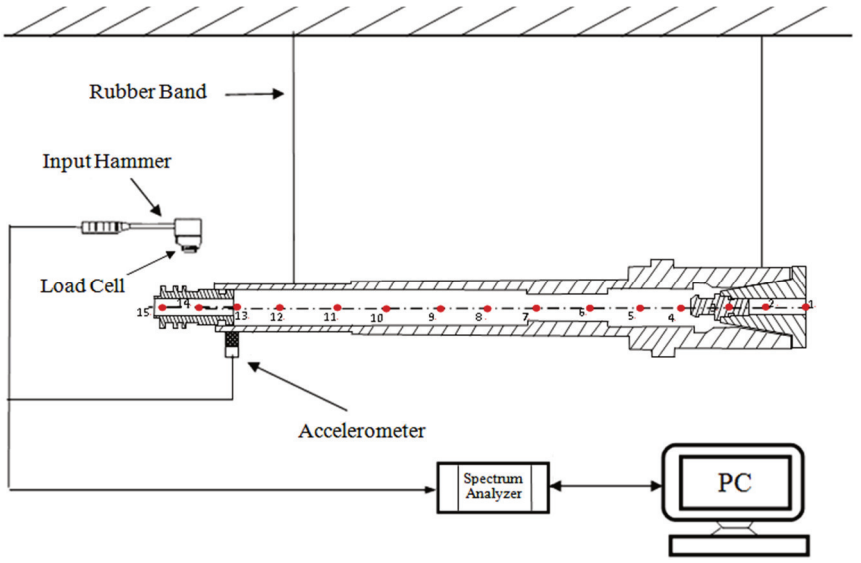

Fig. 3. Schematic of the experimental modal testing apparatus

Also, the maximum speed of the studied commercial spindle is considered in the finite element analysis for understanding the differences of results obtained from the stationary and dynamic analysis, respectively.

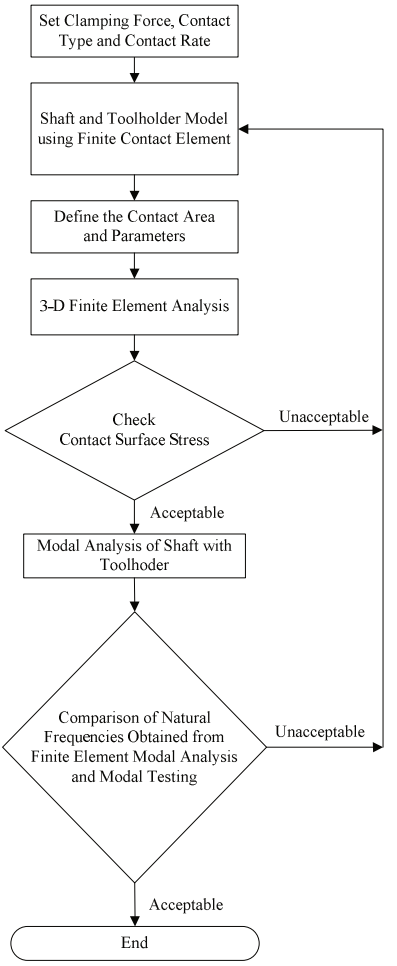

Fig. 4. The flowchart for this study

3. Illustrated actual example and results

In this study, a commercialized 4.6 KW engraving spindle with ATC is studied. The analysis flowchart is shown in Fig. 4. The clamping force, contact type and contact rate are decided firstly. The friction coefficients of steel vs. steel are between 0.029-0.12 obtained by look-up table. In the analysis flow, the first check point is to check, based on engineering practice and common knowledge, the adequacy of calculated contact stress on the contacting surfaces. In light of the geometry and the boundary conditions of the finite element model, some characteristic of the contact stress is expected, such as axisymmetry, uniformity in smoother areas, high stress gradient on load concentrated areas, etc. If inadequacies are observed in the calculations, then the process should be U-turned to the 2nd stage of the analysis flow. For the shaft-toolholder system, it is constructed by rotary shaft, drawbar mechanism and toolholder. The schemes of shaft and toolholder are shown in Fig. 5 and Fig. 6, respectively. Their detailed dimensions are shown in Table 1. The shaft and toolholder are modeling with four one-quarter circle and are manually meshed in a uniform pattern. The detailed meshes of shaft and toolholder can be found in [22].

Furthermore, the drawbar mechanism contains the gripper part, disc springs, and sensing nut and drawbar-rod four components. If all of these components are modeled with solid element, it will take much more computer resources in the analysis stage. Therefore, a hybrid modeling for the drawbar mechanism is proposed herein. The drawbar-rod is individually constructed as 3-D

solid model, and the MASS21 element is utilized for the modeling of the disc springs, sensing nut and gripper part. According to the design chart, the actual measured mass is uniformly applied to the nodes at the surface of drawbar-rod as shown in Fig. 7 (red dots). Therefore, the mass of disc springs is uniformly allocated to 120 points, 24 points for the sensing nut mass, and 24 points for the gripper part mass. The COMBIN14 element is used to simulate the contact status of O-ring between the shaft inner hole and drawbar-rod.

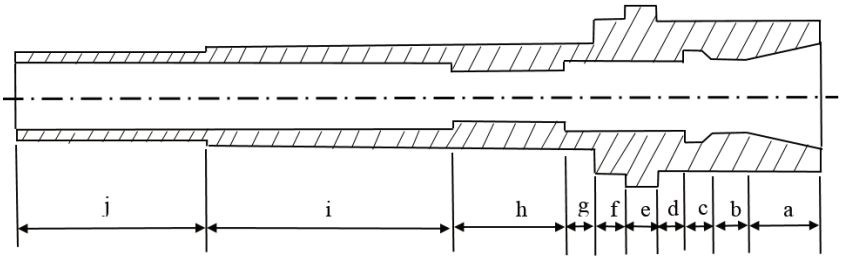

Fig. 5. The design chart of shaft

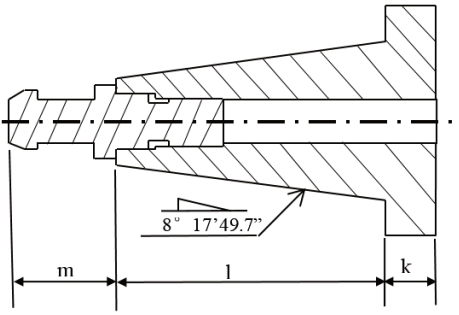

Fig. 6. The design chart of toolholder

Table 1. The dimensions of the studied shaft and toolholder

Location	Dimension		
	Length (mm)	Inner diameter (mm)	Outer diameter (mm)
a	26.057		35
b	11.991	18	35
c	10.952	22	35
d	10.0	17.5	35
e	11.0	17.5	42
f	11.0	17.5	35
g	11.7	17.5	24
h	39.0	12.5	24
i	89.3	15.5	24
j	69	15.5	20
k	8	6.8	37
l	40.5		
m	16		

For the material properties, the Young's modulus of shaft is 2.1×10^{11} N/m^2 and density 7950 kg/m^3. The Poisson's ratio is 0.333. The material properties of toolholder are same as shaft. The contact area is defined after the basic model is established. In the finite element contact analysis, two end surfaces of the sensing nut and toolholder are fixed. The augmented Lagrange method is chosen as solver, contact detection is located at Gauss point. After the contact static analysis, the finite element model with pre-stress is constructed. Then the solver is changed to subspace and finite element modal analysis is conducted.

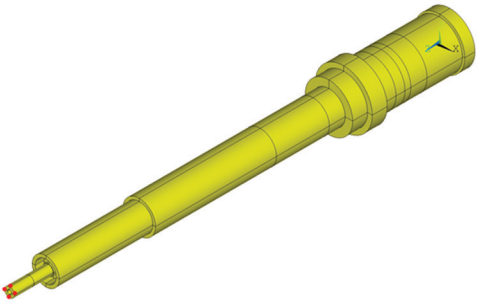

Fig. 7. The drawbar mechanism modeling with hybrid elements

Table 2. Comparison of natural frequencies obtained from experiment modal testing and finite element modal analysis for the shaft-toolholder system with drawbar mechanism

Natural frequency (Hz)		Methods	
		Modal testing	Finite element modal analysis
For shaft-toolholder system with drawbar mechanism	1st ω_n	989	1023
	2nd ω_n	–	1341
	3rd ω_n	–	2135
	4th ω_n	2671	2603

In order to verify the finite element modal analysis results, the experimental modal testing is performed to obtain the natural frequencies of the shaft-toolholder system. The natural frequencies obtained by the two methods are compared as shown in Table 2. The first two natural frequencies obtained from modal testing are 989 Hz and 2671 Hz, respectively and the corresponding natural frequencies obtained from the finite element modal analysis with the hybrid modeling of drawbar mechanism are 1023 Hz and 2603 Hz, respectively. The percentage errors of natural frequencies are less than 4 %. The differences are reasonable and the model can be used for the subsequent analysis. It is noted that, for the finite element modal analysis with the hybrid modeling of drawbar mechanism, the 2nd and 3rd natural frequencies are the natural frequencies of drawbar mechanism. The corresponding mode shapes are shown in Fig. 8 and Fig. 9. It is obvious that natural frequencies of drawbar mechanism will impact on the vibration mode. Therefore, the natural frequencies of drawbar mechanism can be obtained by applying the hybrid modeling.

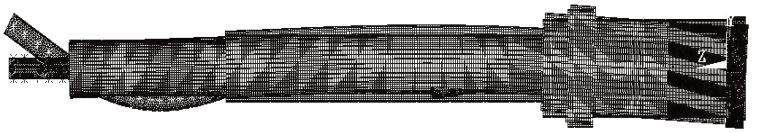

Fig. 8. The mode shape corresponding to the natural frequency 1341 Hz obtained from the finite element modal analysis with the hybrid modeling of drawbar mechanism

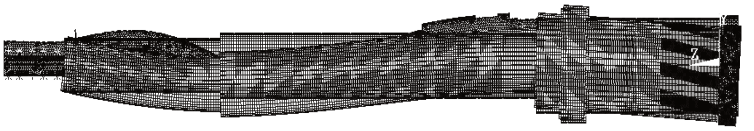

Fig. 9. The mode shape corresponding to the natural frequency 2135 Hz obtained from the finite element modal analysis with the hybrid modeling of drawbar mechanism

In this paper, two different clamping forces, 150 and 250 Kgf, three coefficients of friction, two contact types and four contact rates are investigated. The results of calculated frictional torque with two different clamping forces and rotary speed 0 rpm are shown in Table 3 and Table 4. Furthermore, since the shaft-toolholder system is always operated under a rotating speed, the rotary speed effects will be considered in the analysis. The deformations of shaft-taper hole and

toolholder for contact rate 100 %, coefficient of friction 0.0745, clamping force 150 Kgf, are compared and shown in Fig. 10 and Fig. 11. The comparisons of friction torque with rotating speed 0 and 30,000 rpm are also shown in Table 5. From the results of Figs. 10-11 one can know that the deformations are inconsistent between the shaft-taper hole and toolholder when the spindle speed is taken into account. The deformation of shaft-taper hole is larger than that of toolholder such that the contact condition is changed from complete contact to Type II, i.e., the contact rate and friction torque will be decreasing. For example, the friction torque with $\mu = 0.0745$, clamping force 150 Kgf and contact rate 100 % is 5.16 N·m for 30000 rpm. It is equivalent to the friction torque of contact rate 85 % for 0 rpm (from Table 3).

Table 3. The calculated friction torques with different coefficient of friction, contact type and contact rate (for clamping force 150 Kgf and 0 rpm)

Coefficient of friction (μ)	Contact rate	Contact type	
		Type I	Type II
		Friction torque (N·m)	
0.029	100 %	2.56	
	90 %	2.63	2.55
	80 %	2.69	2.54
	70 %	2.73	2.49
0.0745	100 %	5.20	
	90 %	5.33	5.18
	80 %	5.43	5.13
	70 %	5.55	5.06
0.12	100 %	6.90	
	90 %	7.08	6.87
	80 %	7.25	6.81
	70 %	7.40	6.72

Table 4. The calculated friction torques with different coefficient of friction, contact type and contact rate (for clamping force 250 Kgf and 0 rpm)

Coefficient of friction (μ)	Contact rate	Contact type	
		Type I	Type II
		Friction torque (N·m)	
0.029	100 %	4.27	
	90 %	4.38	4.25
	80 %	4.48	4.23
	70 %	4.55	4.15
0.0745	100 %	8.67	
	90 %	8.88	8.63
	80 %	9.05	8.55
	70 %	9.25	8.43
0.12	100 %	11.50	
	90 %	11.80	11.45
	80 %	12.08	11.35
	70 %	12.33	11.20

Table 5. The comparison of friction torque with rotating speed 0 and 30000 rpm (for contact rate 100 %)

Clamping force (Kgf)	150		250	
Coefficient of friction (μ)	0 rpm	30000 rpm	0 rpm	30000 rpm
	Friction torque (N·m)			
0.029	2.56	2.53	4.27	4.22
0.0745	5.20	5.16	8.67	8.66
0.12	6.90	6.78	11.50	11.45

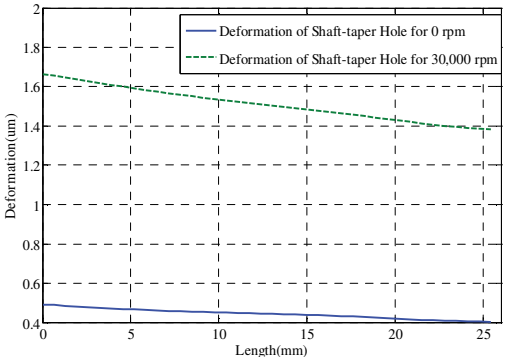

Fig. 10. The deformations of shaft-taper hole with rotating speed 0 and 30000 rpm (for contact rate 100 %, $\mu = 0.0745$, clamping force 150 Kgf)

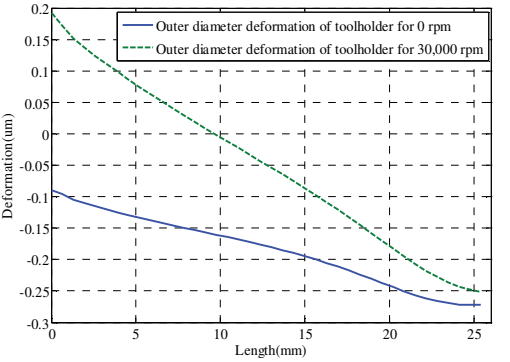

Fig. 11. The deformations of toolholder with rotating speed 0 and 30000 rpm (for contact rate 100 %, $\mu = 0.0745$, clamping force 150 Kgf)

4. Conclusions

In this paper, the contact analysis of shaft-toolholder assembly by using finite contact element is conducted firstly, then the finite element modal analysis of shaft-toolholder assembly with pre-stress is calculated, and the results obtained from finite element modal analysis is verified with those obtained from experimental modal testing for guaranteeing the accuracy of modeling. Finally the results of finite element contact analysis for the frictional torques with different clamping force, coefficient of friction, contact type, contact rate and rotating speed are calculated. Several conclusions can be made as follows:

1. In this study, the modeling for the shaft-toolholder system is proposed. The percentage errors of natural frequencies are all less than 4 %. Therefore, the proposed methodology of modeling for the finite element analysis of the shaft-toolholder assembly is effective and accurate.

2. The contact type and contact rate have significant effects on the friction torque. The non-uniform contact condition of Type I, contact region at larger diameter, will provide larger friction torque to resist the cutting force. This result can be used to the manufacture of toolholder and shaft-taper hole.

3. The deformations are inconsistent between the shaft-taper hole and toolholder when the spindle speed is taken into account, it will cause the contact condition change to Type II, contact region at small diameter, and will has a decrease in the frictional torque. Therefore, the contact condition of Type I is suggested when the toolholder and shaft-taper hole are machined.

Acknowledgement

This support of the National Science Council (NSC) under the Grant No. NSC102-2221-E-269-004 in Taiwan is gratefully acknowledged. Also the authors are grateful to the assistance by Parfaite Company on offering the drawings, parts/components, and working assemblies.

References

[1] **Hughes T. J. R., Taylor R. L., Sackman J. L., Curnier A., Kanoknukulchai W.** A finite element method for a class of contact-impact problems. Computer Methods in Applied Mechanics and Engineering, Vol. 8, 1976, p. 249-276.

[2] **Oysu C., Fenner R. T.** Coupled FEM-BEM for elastoplastic contact problems using Lagrange multipliers. Applied Mathematical Modelling, Vol. 30, 2006, p. 231-247.

[3] **Gonza'lez J. A., Park K. C., Felippa C. A., Abascal R.** A formulation based on localized Lagrange multipliers for BEM–FEM coupling in contact problems. Computer Methods in Applied Mechanics and Engineering, Vol. 197, 2008, p. 623-640.

[4] **Ju S. H., Stone J. J., Rowlands R. E.** A new symmetric contact element stiffness matrix for frictional contact problems. Computers & Structures, Vol. 54, Issue 2, 1995, p. 289-301.

[5] **Ezawa Y., Okamoto N.** Development of contact stress analysis programs using the hybrid method of FEM and BEM. Computers & Structures, Vol. 57, Issue 4, 1995, p. 691-698.

[6] **Ertürk A., Özgüven H. N., Budak E.** Analytical modeling of spindle-tool dynamics on machine tools using Timoshenko beam model and receptance coupling for the prediction of tool point FRF. International Journal of Machine Tools & Manufacture, Vol. 46, 2006, p. 1901-1912.

[7] **Ertürk A., Özgüven H. N., Budak E.** Effect analysis of bearing and interface dynamics on tool point FRF for chatter stability in machine tools by using a new analytical model for spindle-tool assemblies. International Journal of Machine Tools & Manufacture, Vol. 47, 2007, p. 23-32.

[8] **Wock E. H. M., Spachtholz G.** 3- and 4-contact point spindle bearings – a new approach for high speed spindle systems. Manufacturing Technology, Vol. 52, 2003, p. 311-316.

[9] **Hsu M. C., Junz Wang J. J.** Dynamic analysis of milling system with high speed built-in-motor spindle. M. S. dissertation, National Cheng Kung University, Tainan, Taiwan, 2003, (in Chinese).

[10] **Chen H. J., Fang J.** The dynamic analysis for the toolholder mechanism in a build-in spindle. M. S. dissertation, Feng Chia University, Taichung, Taiwan, 2009, (in Chinese).

[11] **Shieh L. C., Lin B. T.** The effects of centrifugal deformation on the high-speed spindle. M. S. dissertation, National Kaohsiung First University of Science and Technology, Kaohsiung, Taiwan, 2002, (in Chinese).

[12] **Wang J. H.** Investigation of the tool holder system with a taper angle 7:24. International Journal of Machine Tools & Manufacture, Vol. 34, Issue 8, 1994, p. 1163-1176.

[13] **Li H., Shin Y. C.** Analysis of bearing configuration effects on high speed spindles using an integrated dynamic thermo-mechanical spindle model. International Journal of Machine Tools & Manufacture, Vol. 44, 2004, p. 347-364.

[14] **Chen C. H., Wang K. W., Shin Y. C.** An integrated approach toward the dynamic analysis of high speed spindles, Part I: System model. Journal of Vibration and Acoustics, Vol. 116, 1994, p. 506-513.

[15] **Chen C. H., Wang K. W., Shin Y. C.** An integrated approach toward the dynamic analysis of high speed spindles, Part II: Dynamics under moving end load. Journal of Vibration and Acoustics, Vol. 116, 1994, p. 514-522.

[16] **Wang J. S., Sun J. H.** Finite element analysis for the put-in force of drawbar mechanism in high speed air spindle. M. S. dissertation, National Kaohsiung First University of Science and Technology, Kaohsiung, Taiwan, 2001, (in Chinese).

[17] **Namazi M., Altintas Y., Abe T., Rajapakse N.** Modeling and identification of tool holder-spindle interface dynamics. International Journal of Machine Tools & Manufacture, Vol. 47, 2007, p. 1333-1341.

[18] **Sun H. T., Su C. T.** Analysis of clamping force and contact pressure of the high speed spindle. M. S. dissertation, National Kaohsiung First University of Science and Technology, Kaohsiung, Taiwan, 2007, (in Chinese).

[19] **Hwang Y. W., Sen C. T.** Type synthesis for tool holding device and design for the power draw bar of spindle. M. S. dissertation, National Chung Cheng University, Tainan, Taiwan, 1997, (in Chinese).

[20] **Chen S. Y., Kung C., Hsu J. C.** Dynamic analysis of a rotary hollow shaft with hot-fit part using contact elements with friction. Transactions of the Canadian Society for Mechanical Engineering, Vol. 35, Issue 3, 2011, p. 461-474.

[21] **Chen S. Y.** The dynamic analyses and verifications of a hollow shaft with hot-fit component using 3D finite contact element. Transactions of the Canadian Society for Mechanical Engineering, Vol. 37, Issue 1, 2013, p. 21-38.

[22] **Chen S. Y., Lin I. F.** Investigation of clamping force for a high-speed shaft with toolholder using contact element analysis. Journal of Vibroengineering, Vol. 16, Issue 3, 2014, p. 1134-1142.